PAPER

Encapsulation of a zinc phthalocyanine derivative in self-assembled peptide nanofibers†

Ruslan Garifullin,‡[a] Turan S. Erkal,‡[a] Sezen Tekin,[b] Bülend Ortaç,[a] Ayşe Gül Gürek,[c] Vefa Ahsen,[c] H. Gul Yaglioglu,*[b] Ayhan Elmali*[b] and Mustafa O. Guler*[a]

In this article, we demonstrate encapsulation of octakis(hexylthio) zinc phthalocyanine molecules by non-covalent supramolecular organization within self-assembled peptide nanofibers. Peptide nanofibers containing octakis(hexylthio) zinc phthalocyanine molecules were obtained *via* a straight-forward one-step self-assembly process under aqueous conditions. Nanofiber formation results in the encapsulation and organization of the phthalocyanine molecules, promoting ultrafast intermolecular energy transfer. The morphological, mechanical, spectroscopic and non-linear optical properties of phthalocyanine containing peptide nanofibers were characterized by TEM, SEM, oscillatory rheology, UV-Vis, fluorescence, ultrafast pump–probe and circular dichroism spectroscopy techniques. The ultrafast pump–probe experiments of octakis(hexylthio) zinc phthalocyanine molecules indicated pH controlled non-linear optical characteristics of the encapsulated molecules within self-assembled peptide nanofibers. This method can provide a versatile approach for bottom-up fabrication of supramolecular organic electronic devices.

1. Introduction

The construction of metal complex chromophores (*e.g.* phthalocyanine and porphyrin) containing nanostructures of well-defined size and shape in water is of great interest because of their attractive photochemical, photophysical and electronic properties.[1] Zinc phthalocyanine complexes are interesting examples of chromophoric molecules. Various methods such as metal coordination, electrostatic interactions, hydrogen bonding and host–guest interactions have been previously utilized to organize phthalocyanine molecules.[2–6]

In this study, we present a straight-forward, one-pot hydrophobic encapsulation method for organizing zinc phthalocyanine derivatives within peptide nanofibers. Our method involves the solvophobic effect along with hydrogen bonding in order to achieve chromophore encapsulation and nanofiber formation. As a result of encapsulation and nanofiber formation, the zinc phthalocyanine molecules are aligned and an ultrafast energy transfer phenomenon is observed upon their organization through the peptide nanofiber core. Several successful attempts to mimic the ultrafast energy transfer mechanism were performed by using polymers,[7] dendrimers,[8] porphyrin arrays linked by covalent bonds[9,10] and by self-assembled systems.[11–13] It is known that the ultrafast energy transfer characteristics of zinc phthalocyanine molecules can be exploited to mimic the light harvesting mechanism in photosynthetic antenna proteins[14,15] and as we observed in this work, it can be tuned with the help of self-assembled peptide nanofibers.

2. Experimental section

Materials

9-Fluorenylmethoxycarbonyl (Fmoc) protected amino acids, Fmoc-Rink Amide MBHA resin, and 2-(1*H*-Benzotriazol-1-yl)-1,1,3,3-tetramethyluronium hexafluorophosphate (HBTU) were purchased from NovaBiochem and ABCR. The other chemicals were purchased from Fisher, Merck, Alfa Aesar or Aldrich and used as received.

Peptide amphiphile (PA) synthesis

Lauryl-VVAGH-Am peptide was constructed on Fmoc-Rink Amide MBHA resin. Amino acid coupling reactions were performed with 2 equivalents of Fmoc-protected amino acid, 1.95 equivalents of HBTU and 3 equivalents of DIEA for 2 h. The Fmoc protecting group removal was performed with 20% piperidine/DMF solution for 25 min. Cleavage of the peptides from the resin was carried out with a mixture of TFA : TIS : H$_2$O in a ratio

[a]UNAM-Institute of Materials Science and Nanotechnology, Bilkent University, Ankara, Turkey 06800. E-mail: moguler@unam.bilkent.edu.tr
[b]Department of Engineering Physics, Ankara University, Ankara, Turkey 06100. E-mail: ayhan.elmali@eng.ankara.edu.tr; gul.yaglioglu@eng.ankara.edu.tr
[c]Department of Chemistry, Gebze Institute of Technology, Gebze, Kocaeli, Turkey 41400
† Electronic supplementary information (ESI) available: additional experimental details. See DOI: 10.1039/c1jm14181c
‡ These authors contributed equally to this work.

This journal is © The Royal Society of Chemistry 2012

J. Mater. Chem., 2012, **22**, 2553–2559 | 2553

of 95 : 2.5 : 2.5 for 2 h. Excess TFA was removed by rotary evaporation. The remaining peptide was triturated with ice-cold diethyl ether and the resulting white precipitate was freeze-dried. The peptide was characterized using an Agilent 1200–6530 quadrupole time of flight (Q-TOF) mass spectrometer with an electrospray ionization (ESI) source equipped with reverse-phase analytical high performance liquid chromatography (HPLC) with a Zorbax SB-C8 4.6 × 100 mm column (Fig. S1). A gradient of 0.1% formic acid/water and 0.1% formic acid/acetonitrile was used as the mobile phase for analytical HPLC.

Octakis(hexylthio) zinc phthalocyanine synthesis

1,2-di(hexylthio)-4,5-dicyanobenzene and octakis(hexylthio) phthalocyaninato zinc(II) were synthesized using the reported procedure.[16] All other reagents and solvents were obtained from commercial suppliers and dried as described in Perrin and Armarego[17] before use. Elemental analyses were obtained using a Thermo Finnigan Flash 1112 Instrument. Mass spectra were obtained using a Bruker MicroTOF LC/MS spectrometer using the electrospray ionization (ESI) method at Gebze Institute of Technology. Infrared spectra were recorded on a Bio-Rad FTS 175C FT-IR spectrophotometer using KBr pellets. Analytical thin layer chromatography (TLC) was performed on silica gel (Merck, Kieselgel 60, 0.25 mm thickness) with F_{254} indicator. Column chromatography was performed on silica gel (Merck, Kieselgel 60, 70–230 mesh; for 3 g crude mixture, 100 g silica gel was used in a column of 3 cm in diameter and 60 cm in length). ^{1}H and ^{13}C NMR spectra were recorded on a Varian INOVA 500 MHz spectrometer using TMS as an internal reference for ^{1}H- and ^{13}C-NMR. UV-Vis spectra were recorded with a Shimadzu 2001 UV spectrophotometer.

UV-Vis spectroscopy and fluorescence measurements

1.24×10^{-6} M octakis(hexylthio) zinc phthalocyanine (ZnPc) in THF solution was prepared and added into a 1 cm quartz cuvette. 3.80×10^{-6} M ZnPc and 3.84×10^{-4} M PA solution was prepared at different pH values and added into a 1 cm quartz cuvette. A solid ZnPc film was prepared by immersing a microscope slide in a solution of ZnPc in THF and letting the sample dry in air. Absorbance measurements were performed on a Varian Cary 5000 UV-Vis-NIR spectrophotometer. Fluorescence measurements were performed on a Varian Cary Eclipse fluorescence spectrophotometer.

Circular dichroism (CD)

A Jasco J-815 CD spectrophotometer was used for CD analysis. Solutions of 3.8×10^{-6} M ZnPc and 3.84×10^{-4} M PA were formed at different pH values.

Scanning electron microscopy (SEM)

SEM imaging was performed with a FEI Quanta 200 FEG scanning electron microscope. Cryo-SEM samples were prepared on a cryo-SEM stage by decreasing the temperature to −15 °C. Samples for standard imaging were drop cast on a silicon wafer and dried in a critical point dryer (Autosamdri-815B, Series C). Dried samples were coated with 6 nm Au/Pd.

Transmission electron microscopy (TEM)

TEM imaging was performed with a FEI Tecnai G2 F30. Diluted samples were placed on a Lacey carbon coated 300 mesh copper grid. 2 wt% uranyl acetate solution was used for staining organic nanostructures. 10 μL of diluted sample solution was dropped on a grid and kept there for 1 min. The excess was removed by pipetting. Then, 20 μL of 2 wt% uranyl acetate solution was put on a parafilm sheet. The grid was placed on the top of the drop with its upper side down and kept there for 5 min. Stained grids were dried in the fume hood at room temperature overnight.

Oscillatory rheology

Rheology measurements were performed with an Anton Paar Physica RM301 Rheometer operating with a 25 mm parallel plate configuration at 25 °C. 300 μL of 3.80×10^{-6} M ZnPc/3.84×10^{-4} M PA and 3.84×10^{-4} M PA solutions were carefully loaded on the center of the lower plate and 2.6 μL of 1 M NaOH solution was added then left untouched for 15 min before measurement. After equilibration, the upper plate was lowered to a gap distance of 0.62 mm. Storage moduli (G') and loss moduli (G'') values were scanned in a strain sweep mode and a shear strain value of 0.4% was found to be optimal; frequency sweep measurements were made with a constant shear strain of 0.4%.

Femtosecond pump–probe measurements

The laser source for the ultrafast pump–probe experiments was a Ti:sapphire laser amplifier–optical parametric amplifier system (Spectra Physics, Spitfire Pro XP,TOPAS). The pulse duration was measured as 100 fs for the experiments. The investigated samples were placed in quartz cuvettes with 1 mm path length. A 690 nm laser was used as a pump beam and white light continuum was used as a probe beam (Spectra Physics, Helios). The UV-Vis absorption spectrum of each sample measured before and after every pump–probe experiment did not show any degradation.

Singlet oxygen measurement

The singlet oxygen generating capability of ZnPc in THF and peptide encapsulated ZnPc in water was performed using singlet oxygen trap molecules 1,3-diphenylisobenzofuran (DPBF) and 2,2′-(anthracene-9,10-diyl)dimalonic acid (ADMA), respectively. A 660 nm emitting 3000 mCd lead source was used as the light source. A solution containing DPBF (74 μM) and ZnPc (50 nM) was prepared in THF. A control solution was prepared with DPBF (74 μM) alone. A 3.80×10^{-6} M solution of ZnPc encapsulated in 3.84×10^{-4} M PA was prepared by the encapsulation process described in the sample preparation section. 115.38 μL of this solution and 5 μL of 1 M HCl solution were added to 1.5 mL of 2.70×10^{-4} M ADMA and the total volume was brought to 3 mL by addition of water. The control solution of ADMA (135 μM) was prepared in H_2O. 2.22×10^{-7} moles of DPBF and 4.44×10^{-10} moles of ZnPc were dissolved in 200 μL THF and mixed with 2.22×10^{-5} moles of PA in 2 mL of water solution to encapsulate both DPBF and ZnPc molecules. The total volume was brought to 3 mL before singlet oxygen measurement. All solutions were aerated for 5 min. Then, the

absorbance spectrum of each solution was taken at 5 min intervals while the solutions were kept in the dark for 15 min. After 15 min samples were exposed to 660 nm light from 4 cm distance for a total period of 35 min and the absorbance was recorded at 5 min intervals for each solution.

Sample preparation

The PA is an amphiphilic molecule, which helps to solubilize ZnPc molecules in water by means of encapsulation driven by the hydrophobic effect. Three mg of ZnPc was dissolved in 2 mL of THF to obtain a stock solution. ZnPc solution was diluted 800 times prior to UV-Vis and fluorescence spectroscopy measurements. ZnPc with PA solution was prepared by mixing 700 μL of 1 mM ZnPc stock solution with 7 mL of 10 mM PA solution (45.42 mg of PA in 7 mL of water). This mixture was ultrasonicated for 45 min. ZnPc with PA solution was diluted 26 times prior to UV-Vis and fluorescence spectroscopy, SEM, TEM, and CD characterizations. The ZnPc thin film was prepared by immersing microscope slide into concentrated ZnPc in THF solution and the sample was air dried.

3. Results and discussion

Here, we report the encapsulation and non-covalent alignment of octakis(hexylthio) zinc phthalocyanine (ZnPc) molecules (**1**) by using a self-assembling peptide amphiphile (PA)[18,19] molecule (**2**) with the sequence of Lauryl-VVAGH-Am (Figs 1, S1 and S2†). Encapsulation of the zinc phthalocyanine derivative is performed by hydrophobic interactions between alkylthiol functionalized ZnPc and the fatty acid conjugated peptide molecule (Fig. 1). The peptide amphiphile molecules render ZnPc molecules soluble in water. The histidine residue provides hydrophilic property to the amphiphilic peptide molecules. The nature of the histidine residue determines the self-assembly properties of the PA molecule depending on the pH of the environment. During the encapsulation process, the ZnPc molecule was dissolved in THF and the PA molecule was dissolved in water. These two solutions were mixed together and the mixture was ultrasonicated for encapsulation of ZnPc molecules within the peptide nanofibers during evaporation of THF. At the end of the encapsulation process, ZnPc molecules were surrounded by the PA molecules (Fig. 1) which can self-assemble into nanofibers with a hydrophobic core.[20]

3.1 Morphological characterizations

In this study, hydrophobic ZnPc molecules were located in the hydrophobic core of the self-assembled PA nanofibers due to hydrophobic interactions. The morphology of the self-assembled nanostructures was studied by means of scanning and transmission electron microscopy techniques. It was observed that mixture of ZnPc and PA yields one-dimensional fibrous nanostructures. SEM and TEM images of the ZnPc-containing peptide nanofibers are shown in Figs 2, S3 and S4.† In order to verify the presence of ZnPc molecules within the peptide nanofibers, an energy dispersive X-ray spectrum demonstrating the presence of zinc was recorded from an individual peptide nanofiber (Fig. S6†). The singlet oxygen generation capacity of the ZnPc molecules was measured to confirm the encapsulation of ZnPc molecules within the PA nanofibers. The ZnPc molecule and DPBF (a singlet oxygen trap molecule) were dissolved in THF and trap molecule degradation was observed upon irradiation with an appropriate light source. The peptide encapsulated ZnPc sample was mixed with a water soluble singlet oxygen trap molecule (ADMA) and again irradiated, however no detectable trap molecule degradation was observed. Based on this observation, ZnPc molecules do not accumulate on the surface of the nanofibers and do not dissolve in the aqueous solution. The ZnPc molecules were co-encapsulated with DPBF molecules, which are soluble in THF and not in water. Upon irradiation of this solution, we observed degradation of the DPBF molecules. Briefly, singlet oxygen generation and consequent trap molecule degradation were observed only in cases of direct interaction between the ZnPc and trap molecule (Figs 3, and S7–S9†). This observation supports the idea of encapsulation of the ZnPc molecules in the hydrophobic core of the peptide nanofibers.

A three-dimensional network of the ZnPc-containing peptide nanofibers forms a self-supporting gel at pH 8 upon neutralization of the charges on the peptide sequence. The mechanical properties of the gels were characterized by oscillatory rheology experiments (Figs S10–S13†). The storage modulus of ZnPc-containing peptide gel is greater than that of the peptide only gel; it can be indirectly inferred that self-organized π-stacks of
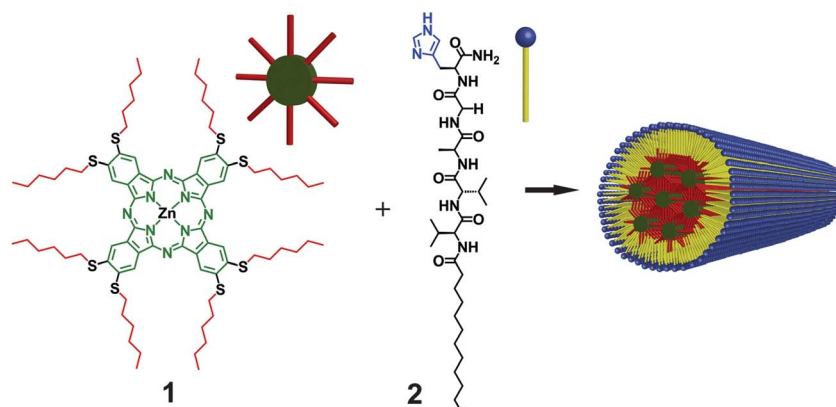

Fig. 1 A schematic representation of ZnPc (**1**) encapsulation in PA (**2**) nanostructures.
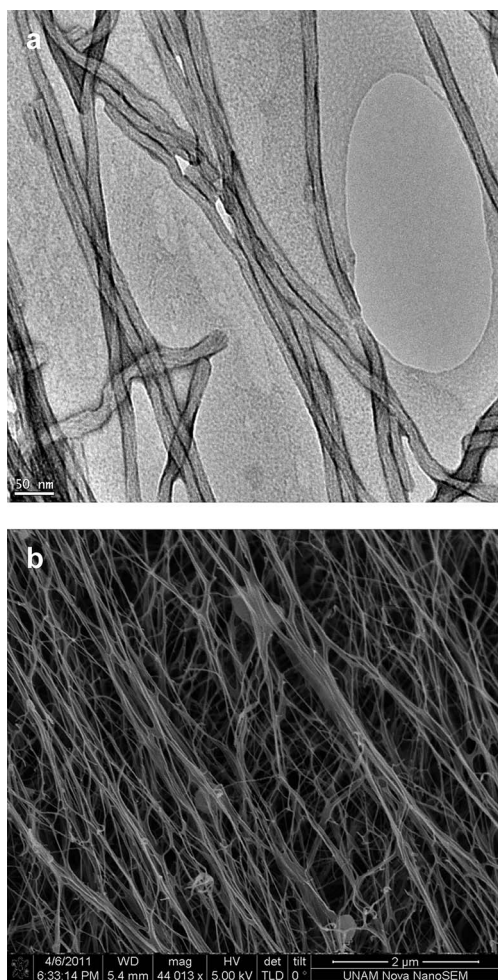
Fig. 2 TEM (a) and SEM (b) images of the ZnPc-containing PA nanostructures.
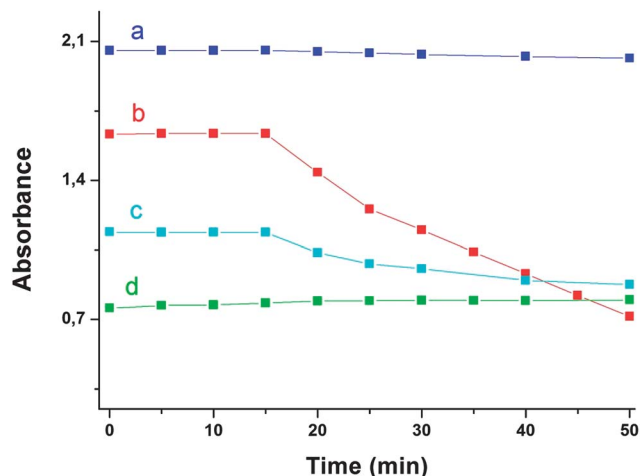
phthalocyanines enhance the mechanical properties of the gel. The cryo-SEM technique revealed the peptide network in aqueous solution (Fig. S14†). The critical point dried gels of PA and ZnPc-containing peptide nanofibers were studied by SEM. Well-defined nanofiber networks were observed for both samples (Figs 2 and S5). The morphology of the nanofibers was also studied by circular dichroism spectroscopy, indicating that the self-assembly process involves an extended β-sheet structural motif (Figs 4 and S15†).

3.2 Spectroscopic characterization

Due to the increase in the local concentration of ZnPc molecules in the core of the peptide nanofibers upon the hydrophobic encapsulation process, the interactions between ZnPc molecules were enhanced and we observed remarkable changes in the spectroscopic properties of the ZnPc molecules. There is a significant difference between the UV-Vis spectrum of ZnPc molecules dissolved in THF and ZnPc with PA molecules in water (Fig. 5). The difference in the absorption bands is caused by aggregation of the ZnPc molecules within the PA nanofibers under aqueous conditions.[21] Encapsulation of ZnPc molecules causes a shift and broadening of the absorption bands.[5,21] The Q-band absorption of ZnPc in THF blue-shifts from 705 to 674 nm compared to ZnPc with the peptide solutions. A smaller blue-shift was observed for the sample at pH 2 compared to samples at pH 5 and pH 8 because of the formation of extended peptide nanostructures at higher pH (Fig. 5). The observed blue-shifts in the Q-band absorption of encapsulated ZnPc upon aggregation in the peptide nanofibers may be caused by formation of H-aggregates (face to face aggregates)[22–24] with effective π–π interactions. However, the mechanism of chromophore aggregation should be characterized in more detail. It is important to compare the spectroscopic behavior of encapsulated chromophores with chromophores in the solid phase because the former ones are completely isolated from the solvent and can resemble the latter ones. For this purpose, a ZnPc thin film was prepared by immersing microscope slide into concentrated ZnPc in THF
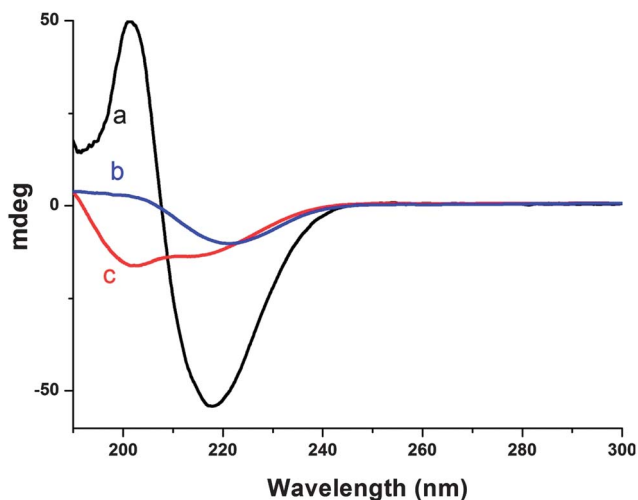

Fig. 3 Singlet oxygen measurements of ZnPc in THF, DPBF in THF, ZnPc within PA in water, ZnPc and DPBF within PA in water. a) DPBF in THF (at 414 nm), b) DPBF + ZnPc in THF (at 414 nm), c) ZnPc + DPBF with PA in water (at 418 nm), and d) ZnPc + PA with ADMA in water (at 381 nm).

Fig. 4 Circular dichroism spectra of ZnPc with PA at pH 2, pH 5, and pH 8; a) ZnPc + PA at pH 2, b) ZnPc + PA at pH 5, and c) ZnPc + PA at pH 8.
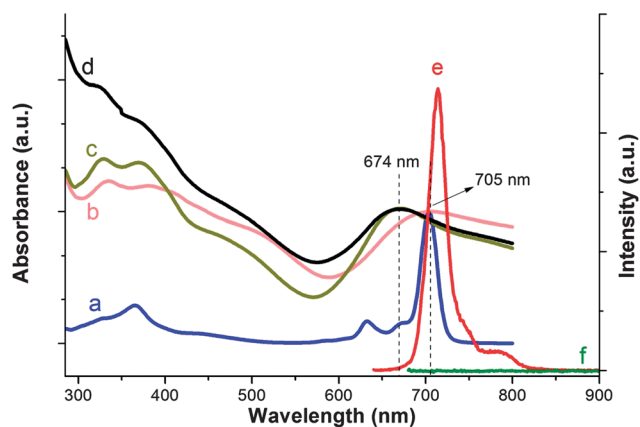
Fig. 5 Absorbance and fluorescence emission spectra of ZnPc with and without the PA molecules. a) ZnPc absorbance in THF, b) ZnPc with PA absorbance in water at pH 2, c) ZnPc with PA absorbance in water at pH 5, d) ZnPc with PA absorbance in water at pH 8, e) ZnPc fluorescence in THF, and f) ZnPc with PA fluorescence in water.

Fig. 6 Time evolution of the excited state absorption signal at 585 nm of ZnPc under aqueous conditions with PA at different pH values.

solution. The absorption around 670 nm for the ZnPc thin film prepared on a microscope slide surface provided some information about the aggregation state of the chromophoric units in peptide nanofibers (Fig. S16†) analogous to the blue-shifted peaks at around 670 nm for peptide encapsulated ZnPc samples. Encapsulated ZnPc molecules in the nanofiber form revealed solid-like behaviour similar to the ZnPc film. Furthermore, fluorescence spectra of ZnPc in THF (Fig. S20†) and in water with PA molecules (Figs S21 and S22†) differ significantly because of the effect of aggregation and change in the environment of the ZnPc molecules. Interestingly, encapsulation of the ZnPc molecules in the peptide nanofibers results in quenching of the fluorescence emission (Figs 5, S21, and S22†). The fluorescence quenching caused by aggregation was observed for the ZnPc film as well (Figs S17–S19†). The polarity and nature of the environment such as solvent, pH, and temperature are known to have an impact on photophysical properties of fluorescent molecules.[25,26] The UV-Vis spectra at different pH values indicate the indirect effect of pH on the photophysical properties of the ZnPc molecules (Fig. 5). The change in the pH directly affects the polarity and the self-assembly behavior of the PA molecules because of the presence of the histidine residue.

The significant fluorescence quenching observed for encapsulated ZnPc samples can potentially yield fast excited state relaxations due to non-radiative energy transfers between aggregated molecules.[27] In order to study the relationship between the aggregation phenomenon and excited state life time of the chromophores in the peptide nanofibers, ultrafast pump–probe experiments were utilized (Figs S23–S28†). The time evolution of excited state absorption (ESA) signals for ZnPc molecules in THF (Fig. S23†) revealed long-lived excited state relaxation (on the order of ns). On the other hand, the time evolution of ESA signals for peptide encapsulated ZnPc samples (Fig. 6) exhibited very short-lived (on the order of ps and less) excited state relaxation depending on the pH (Table 1).

The transient absorption of ZnPc samples for various time delays is shown in Fig. 7. The ESA signal around 570 nm (T_1
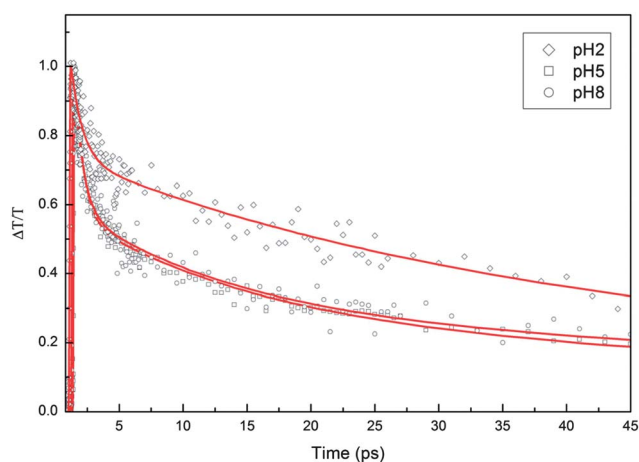
$\rightarrow T_n$ transition) observed for ZnPc in THF decays until 100 ps, then it increases gradually (Fig. 7a). The ground state bleach and stimulated emission (SE) signal at 695 nm at earlier time delays shift to 720 nm after a couple of ps time delay due to the Stokes shift of ZnPc in THF. The excited state at various time delays for ZnPc in peptide nanofibers is shown in Fig. 7b, c and d. A strong scattering signal appears at 690 nm pump wavelength (gray area in Fig. 7) due to the peptide nanofibers. The pump–probe results as a function of wavelength for encapsulated ZnPc at different pH values (Figs S25–S27†) also differ from ZnPc in THF (Fig. S24†). The ESA signal with a long decay time corresponds to transitions between triplet states ($T_1 \rightarrow T_n$ ESA (Fig. S24B†)) of ZnPc in THF (Fig. S24†).[28] A long decay time was not observed in peptide encapsulated ZnPc samples because of the intermolecular fast energy transitions (Figs S25–S27†).[27] Similar behavior was also observed in several studies with zinc phthalocyanines at high concentrations or with zinc phthalocyanine thin films.[29–32] In addition, a strong stimulated emission signal observed for ZnPc in THF at 720 nm was not observed in peptide encapsulated ZnPc samples, which is consistent with the fluorescence quenching observed in the peptide samples (Figs S21 and S22†).

Pump–probe experiment results also revealed the effect of pH on ZnPc in the peptide nanofibers. The pH 2 sample shows the slowest decay time, while samples at pH 5 and pH 8 showed similar faster decay times. Based on this observation, it can be inferred that encapsulation of ZnPc in peptide nanofibers not only yields ultrafast energy transfer between chromophores but also provides a route to control the ultrafast decay time by altering the pH of the solution.

Table 1 Non-linear absorption decay time constants for ZnPc samples at different pH values

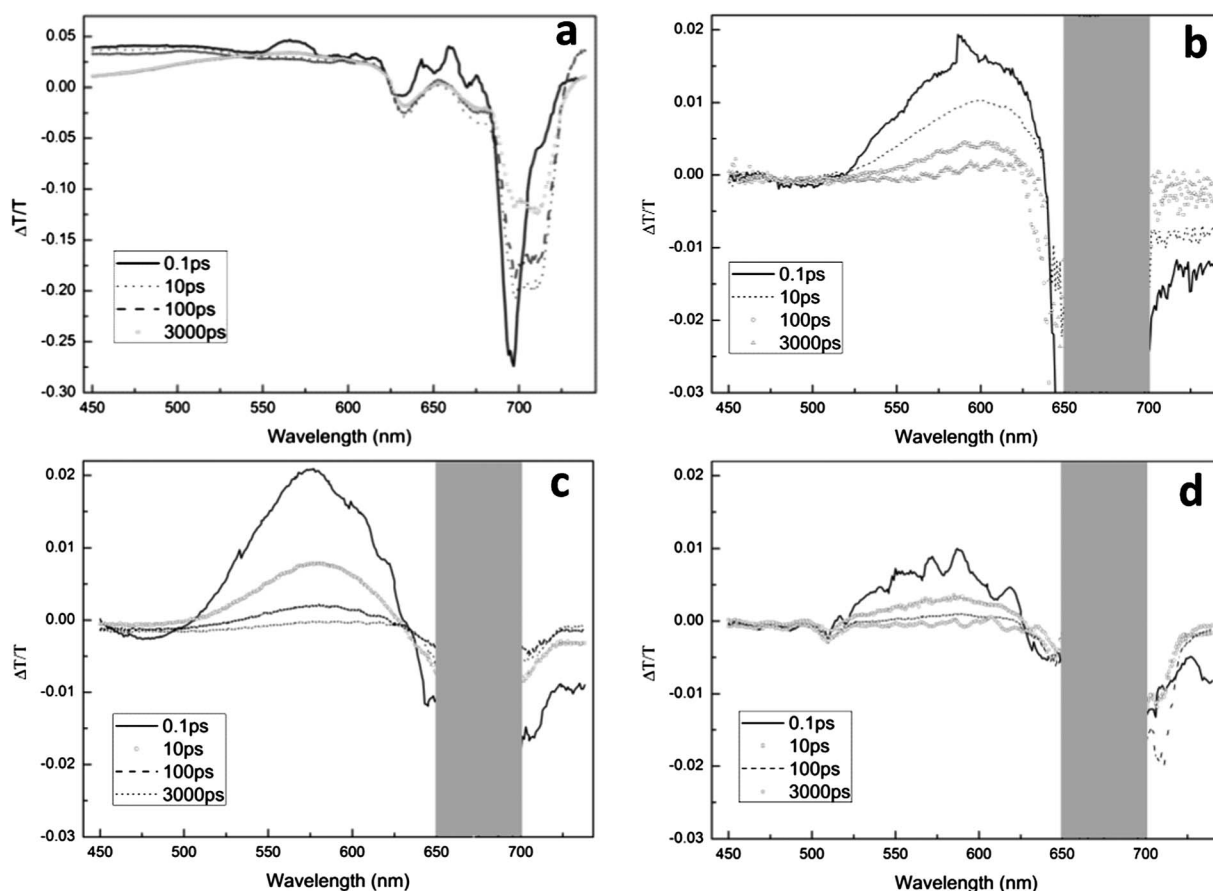| Medium	t_1 (ps)	t_2 (ps)	t_3 (ps)
pH 2	142	33	0.92
pH 5	80	6	0.48
pH 8	100	6	0.47

Fig. 7 Transient spectra of ZnPc. In THF (a), in H_2O with PA at pH 2 (b), at pH 5 (c), at pH 8 (d).

4. Conclusions

In summary, encapsulation of zinc coordinated phthalocyanines by peptide amphiphile molecules was achieved under aqueous conditions. The encapsulation process significantly modifies the photophysical properties of the ZnPc molecule and enables pH controlled ultrafast intermolecular energy transfer. The energy transfer mechanism suggests that these systems can be used to mimic light harvesting photosynthetic antenna proteins. Biologically relevant peptide amphiphiles[33] can provide a myriad of useful applications such as bio-imaging and medical applications when combined with the properties of various chromophores. This method can also provide a versatile approach for bottom-up fabrication of supramolecular organic electronic devices.

References

1 M. Fathalla, A. Neuberger, S.-C. Li, R. Schmehl, U. Diebold and J. Jayawickramarajah, *J. Am. Chem. Soc.*, 2010, **132**, 9966–9967.
2 R. C. George, M. Durmus, G. O. Egharevba and T. Nyokong, *Polyhedron*, 2009, **28**, 3621–3627.
3 S.-C. Suen, W.-T. Whang, F.-J. Hou and B.-T. Dai, *Org. Electron.*, 2006, **7**, 428–434.
4 A. Lützen, S. D. Starnes, D. M. Rudkevich and J. Rebek, *Tetrahedron Lett.*, 2000, **41**, 3777–3780.
5 P. Ma, Z. Bai, Y. Gao, Q. Wang, J. Kan, Y. Bian and J. Jiang, *Soft Matter*, 2011, **7**, 3417–3422.
6 M. K. Khan and P. Sundararajan, *Chem.–Eur. J.*, 2011, **17**, 1184–1192.
7 S. E. Webber, *Chem. Rev.*, 1990, **90**, 1469–1482.
8 J. M. J. Fréchet, *J. Polym. Sci., Part A: Polym. Chem.*, 2003, **41**, 3713–3725.
9 H. Imahori, *J. Phys. Chem. B*, 2004, **108**, 6130–6143.
10 J. Li, A. Ambroise, S. I. Yang, J. R. Diers, J. Seth, C. R. Wack, D. F. Bocian, D. Holten and J. S. Lindsey, *J. Am. Chem. Soc.*, 1999, **121**, 8927–8940.
11 R. Takahashi and Y. Kobuke, *J. Am. Chem. Soc.*, 2003, **125**, 2372–2373.
12 T. van der Boom, R. T. Hayes, Y. Zhao, P. J. Bushard, E. A. Weiss and M. R. Wasielewski, *J. Am. Chem. Soc.*, 2002, **124**, 9582–9590.
13 X. Chen and C. M. Drain, *Enc. Nanosci. Nanotech.*, 2004, **9**, 593–616.
14 R. van Grondelle, J. P. Dekker, T. Gillbro and V. Sundstrom, *Biochim. Biophys. Acta, Bioenerg.*, 1994, **1187**, 1–65.
15 V. Sundström, T. Pullerits and R. van Grondelle, *J. Phys. Chem. B*, 1999, **103**, 2327–2346.
16 A. G. Gürek and Ö. Bekaroğlu, *J. Chem. Soc., Dalton Trans.*, 1994, 1419–1423.
17 D. D. Perrin and W. L. Armarego, *Purification of Laboratory Chemical, 2nd ed.*, Pergamon Press, Oxford, 1980.

18 S. Toksoz, R. Mammadov, A. B. Tekinay and M. O. Guler, *J. Colloid Interface Sci.*, 2011, **356**, 131–137.

19 H. Cui, M. J. Webber and S. I. Stupp, *Biopolymers*, 2010, **94**, 1–18.

20 H. Jiang, M. O. Guler and S. I. Stupp, *Soft Matter*, 2007, **3**, 454–462.

21 W. Liu, T. Jensen, F. Fronczek, R. Hammer, K. Smith and M. Vicente, *J. Med. Chem.*, 2005, **48**, 1033–1041.

22 M. Kasha, H. R. Rawls and A. El-Bayoumi, *Pure Appl. Chem.*, 1965, **11**, 371–392.

23 X. Li, L. E. Sinks, B. Rybtchinski and M. R. Wasielewski, *J. Am. Chem. Soc.*, 2004, **126**, 10810–10811.

24 M. Brasch, A. s. de la Escosura, Y. Ma, C. Uetrecht, A. J. R. Heck, T. s. Torres and J. J. L. M. Cornelissen, *J. Am. Chem. Soc.*, 2011, **133**, 6878–6881.

25 T. Kikteva, D. Star, Z. Zhao, T. L. Baisley and G. W. Leach, *J. Phys. Chem. B*, 1999, **103**, 1124–1133.

26 M. Berezin and S. Achilefu, *Chem. Rev.*, 2010, **110**, 2641–2684.

27 Y. S. Nam, T. Shin, H. Park, A. P. Magyar, K. Choi, G. Fantner, K. A. Nelson and A. M. Belcher, *J. Am. Chem. Soc.*, 2010, **132**, 1462–1463.

28 J. Savolainen, D. van der Linden, N. Dijkhuizen and J. Herek, *J. Photochem. Photobiol., A*, 2008, **196**, 99–105.

29 L. Howe and J. Zhang, *J. Phys. Chem. A*, 1997, **101**, 3207–3213.

30 V. Gulbinas, M. Chachisvilis, L. Valkunas and V. Sundström, *J. Phys. Chem.*, 1996, **100**, 2213–2219.

31 J. Zhou, J. Mi, R. Zhu, B. Li and S. Qian, *Opt. Mater.*, 2004, **27**, 377–382.

32 J. Mi, L. Guo, Y. Liu, W. Liu, G. You and S. Qian, *Phys. Lett. A*, 2003, **310**, 486–492.

33 A. J. van Hell, M. M. Fretz, D. J. A. Crommelin, W. E. Hennink and E. Mastrobattista, *J. Controlled Release*, 2010, **141**, 347–353.